J Mater Sci: Mater Med (2006) 17:795–802
DOI 10.1007/s10856-006-9837-y

Gelation under dynamic conditions: A strategy for *in vitro* cell ordering

Ernesto Doncel-Pérez · Margarita Darder · Eduardo Martín-López · Luis Vázquez · Manuel Nieto-Sampedro · Eduardo Ruiz-Hitzky

Received: 29 December 2004 / Accepted: 21 October 2005

Abstract Ordered gelation under spin-coating conditions, as reported here, is a suitable method to order cells in biogels. Cell ordering is of great importance for functional repair of central nervous system (CNS) injuries, because therapies must include strategies to bridge chystic gaps and facilitate axon growth towards its target. Organized biocompatible and biodegradable substrates may be used for this purpose, to supply trophic support and provide directional cues for neuronal process outgrowth. Atomic force microscopy (AFM) and low temperature scanning electron microscopy (LTSEM), confirmed that fibrils in κ–carrageenan/chitosan and fibrin hydrogels prepared under spin-coating conditions, were longitudinally arranged. The cell model was conveniently tested using rat C6 glioma cells. C6 cells were distributed regularly in fibrin gels formed under centrifugal force. The ability of ordered fibrin scaffolds to promote uniform distribution of transplanted cells, was confirmed by fluorescence microscopy.

E. Doncel-Pérez (✉)
Unidad de Neurología Experimental, CSIC, SESCAM, Hospital Nacional de Parapléjicos, Finca "La Peraleda" s/n, 45071 Toledo, Spain
e-mail: edoncel@cajal.csic.es

M. Nieto-Sampedro
Unidad de Neurología Experimental, CSIC, SESCAM, Hospital Nacional de Parapléjicos, Finca "La Peraleda" s/n, 45071 Toledo, Spain; Departamento de Plasticidad Neural, Instituto Cajal, CSIC, Doctor Arce 37, 28002 Madrid, Spain

M. Darder · L. Vázquez · E. Ruiz-Hitzky
Instituto de Ciencia de Materiales de Madrid, CSIC, Cantoblanco, 28049 Madrid, Spain

E. Martín-López
Departamento de Plasticidad Neural, Instituto Cajal, CSIC, Doctor Arce 37, 28002 Madrid, Spain

1. Introduction

Brain and spinal cord lesions have an increasing social and economic importance in developed countries. Accidents are the major cause of death in adults (only surpassed by heart disease and cancer) and lesions surpass all other problems in number of potential years of life and work lost, because they occur most frequently to people under 45 years of age. About 10 people in a million suffer spinal cord lesions in Spain, most of them (81%) traumatic [1] and no treatment has been described that reliably restores sensorimotor and visceral functions. The best we can do, after vital stabilization, is to teach patients to live as well as possible with the consequences of the lesion.

Injured CNS axons fail to regenerate and reconnect with their targets for several reasons, including the neurite inhibitory properties of the glial environment [2–4] and the intrinsic lack of growth capacity of CNS fibers [5]. A possible approach to promoting target-oriented growth of nerve fibers is the development of organized substrates capable of supplying both, trophic support and guiding cues. Biocompatible and biodegradable three-dimensional scaffolds, both natural and synthetic, have been developed that act as templates to guide tissue growth for injury repair [6, 7]. The repair of spinal cord injury includes strategies to bridge chystic gaps, thus facilitating axon growth towards their targets [8]. Scaffolds of high porosity and surface area, with suitable mechanical properties and specific three-dimensional shape, must be designed for this objective. Materials tested for the purpose of inducing oriented neurite outgrowth include hydrogel

matrices [9, 10], laminin-coated poly(L-lactide) filaments [11] and longitudinally oriented fibrin [12, 13] or collagen gels [14–16].

Transplants of cultured cells, particularly of olfactory ensheathing cells (OECs) [17–21], have been used as a complementary approach. The reported controversial results probably depend on the importance of achieving a uniform distribution of the transplanted cells in the host tissue, reducing cell aggregation and providing a suitable substrate for correct cellular interactions. Forced arrangement of fibrils in a cell containing gel may facilitate oriented growth of transplanted cell processes. We describe here ordered gelation under spin-coating conditions, a method to order cells in biogels. The method yielded highly transparent hydrogels that may be used as cellular bridges to repair CNS lesions.

2. Materials and methods

2.1. Cell culture

A 5% CO_2 humid chamber (at 37°C) was used for cell culture. The C6 rat glioma line was maintained in Dulbecco's modified Eagle medium (DMEM; Sigma, Steinheim, Germany) plus 10% fetal calf serum (Cultek, Madrid, Spain).

Fibrinogen (10 mg/ml) (Sigma, Steinheim, Germany) aliquots were dialyzed at 4°C against Tris-buffered saline (TBS), at pH 7.2 or pH 10. C6 cells (3×10^6) suspended in 400 μl of TBS in 35 mm cell culture plates (Nunc, Denmark) were mixed with 2 ml fibrinogen solution, 10 mM in $CaCl_2$. A solution of thrombin (Sigma, Steinheim, Germany; 1 unit NIH) in TBS (100 μl) was added to obtain 4 mg/ml fibrin gels. The mixture was incubated for 1 h at 37°C and 2 ml DMEM containing 10% FCS was added to terminate the reaction.

2.2. Preparation of fibrin gel oriented under dynamic conditions

Fibrin gels were prepared for atomic force microscopy and scanning electron microscopy studies as follows. A solution of fibrinogen in TBS, pH 7.0 (2 ml of 32 mg/ml), containing 10 mM $CaCl_2$, was placed in a 35 mm Petri dish, at 37°C, under a spin rate of 450 rpm, using a Single Wafer Spin Processor (model WS-400A-6 NPP/LITE SHOWN, from Laurell Technologies Corporation, North Wales, PA). Thrombin (4 U NIH) solution (100 μl) in TBS, pH 7.0, was added to initiate gelation and the gel was spun at 450 rpm for 10 minutes. The same procedure was followed for the preparation of fibrin gel at pH 10.0, using fibrinogen (32 mg/ml) and thrombin (4 units NIH) solutions in TBS, pH 10.0.

2.3. Preparation of oriented. κ-carrageenan/chitosan polyelectrolyte complex gel

High molecular weight chitosan (average MW = 342500 g.mol^{-1}) was supplied by Aldrich and κ-carrageenan (type I, from Irish Moss) by Sigma. κ-carrageenan solution (1% w/v) was prepared in hot bidistilled water, at ca. 70°C, under strong magnetic stirring. Chitosan solution (2 ml; 1% w/v), prepared in 1% (v/v) acetic acid, was added to a 38 mm diameter dish and spun at 450 rpm in the Spin Processor. Under such conditions 2 ml of hot κ-carrageenan solution were added to the dish containing the chitosan and the mixture was kept under a spin rate of 450 rpm for 5 minutes. For comparison, a disordered κ-carrageenan/chitosan gel was prepared using the same starting polysaccharides solutions and mixing them under conventional magnetic stirring. Both kind of samples, prepared under spin-coating and magnetic stirring conditions, were mounted on microscope slides and dried at 60°C for a previous study by means of an optical microscope (Motic B3 Professional Series).

2.4. Viability assay

The C6 glioma cells were plated at 5000 or 10000 cell per well on microtitulation plates and incubated in DMEM-10% FCS for 6 hours to permit adherence. The medium was aspirated and 60 μl of: TBS at pH 10, TBS pH 7, PBS (Negative control) or DMEM-10% FCS (Positive control) were added, 8 replicates per experimental variant were assayed. After 1.15 hours of incubation at 37°C in humid chamber 170 μl DMEM-10% FCS were added. The viability of cells were determined at 24 and 72 h by Vybrant MTT Proliferation Assay Kit (Molecular Probes, Leiden, The Netherlands) following the manufacturer instructions. The changes in absorbance at 595 nm were detected by Titertek Multiskan Plus (Labsystem, Finland).

2.5. Inclusion of cells in an oriented fibrin gel

C6 glioma cells (3×10^6) diluted in TBS, pH 10, were pipetted in the middle of a cell culture plate containing a prewarmed fibrinogen solution (4 mg/ml final concentration) under the spin rate conditions described above. When the cells formed a homogeneous ring, gelation was started by adding thrombin (4 units NIH in 100 μl of TBS pH 10.0). The gel was stirred at 450 rpm for 10 minutes, the oriented cell bearing gel was incubated at 37°C for 1 h and DMEM-10% FCS (2 ml) was added. The plate was finally incubated at 37°C in 5% CO_2 atmosphere for 12 hours and observed by contrast and fluorescence microscopy.

2.6. Atomic force microscopy imaging

Samples of the κ-carrageenan/chitosan polyelectrolyte complex gel and fibrin gels were cut and just deposited on a freshly exfoliated mica substrate for atomic force microscopy (AFM) imaging. AFM measurements were performed after the gel samples were dried. Images were obtained with a Nanoscope IIIa microscope (Digital Instruments, Veeco, Santa Barbara, CA) operating in tapping mode, using the piezoscanner J and using silicon cantilevers. Wide scans (up to 100 μm scan size) were initially made in order to locate the fibrils, which were then imaged at a higher resolution.

2.7. Low Temperature Scanning Electron Microscopy (LTSEM)

Small fragments from each sample were cut with a razor blade and fixed onto the specimen holder of a cryotransfer system with cryo-glue (O.C.T. compound Gurr from BDH Laboratories, Poole, U.K.) at room temperature. The fragments were immediately plunged-frozen in liquid nitrogen and transferred directly into the cryochamber, precooled to -180°C with an air-lock transfer device. The frozen fragments were then fractured with a cooled blade and an etching process was applied by slowly heating the chamber to -90°C over a 2 min period. This process allows sublimation of the first superficial microns of water. The etched fragment was returned to the cryo-chamber, sputter-coated with gold for 2 min 15 s at 10 mA, moved to the SEM-chamber precooled to -150 to -160°C and observed at an acceleration voltage of 10–15 kV. The instrument used was a CT 1500 Cryotrans system (Oxford Instruments) mounted on a Zeiss DSM-960 microscope.

2.8. Fluorescence microscopy

Cell culture plates containing fibrin gels plus C6 cells labelled with Hoechst 33342, (10 μg/ml; Sigma Chem. Co., Steinheim, Germany) were examined on a Zeiss Axiovert 35 microscope fitted with a Nikkon Coolpix 4500 digital camera adjusted for phasecontrast and fluorescence analysis.

3. Results and discussion

3.1. κ-Carrageenan/chitosan polyelectrolyte complex gel prepared under dynamic conditions

The procedure of gelation under dynamic conditions was initially assayed by applying a centrifugal force during the gelation of a mixture of two polysaccharides, chitosan and κ-carrageenan. Both are polyelectrolytes with opposite ionic charges and interact electrostatically giving rise to a polyelectrolyte complex gel [22, 23]. The appearance of the gel depends on the conditions applied during the gelation step. An opaque gel is formed when gelation takes place under conventional magnetic stirring. In contrast, gels formed under centrifugal force, are completely transparent. Whereas a heterogeneous gel was formed under static conditions, transparent and stable complex gels could be prepared under dynamic conditions, without the usually required addition of salts to the starting biopolymer solutions [22, 23].

In order to assess the effect of the centrifugal force on the orientation of the fibrils, we have performed a systematic optical microscopy characterization of both samples, the spin-coated ones (Fig. 1 a–c) and those prepared under conventional magnetic stirring (Fig.1 d–f). The comparison

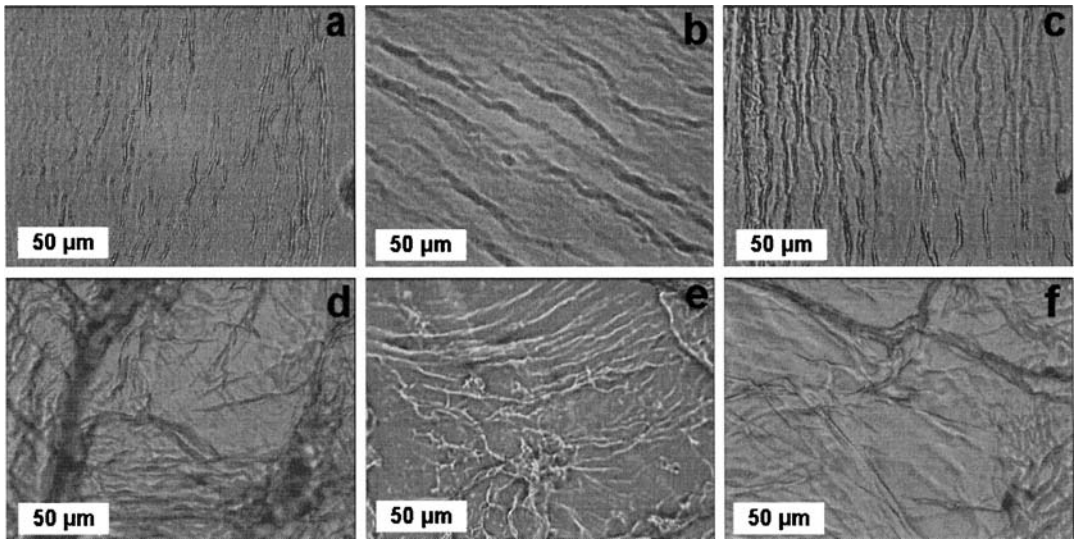

Fig. 1 Optical microscopy images of κ-carrageenan/chitosan polyelectrolyte complex gels prepared under a spin rate of 500 rpm (a–c) and under magnetic stirring (d–f).

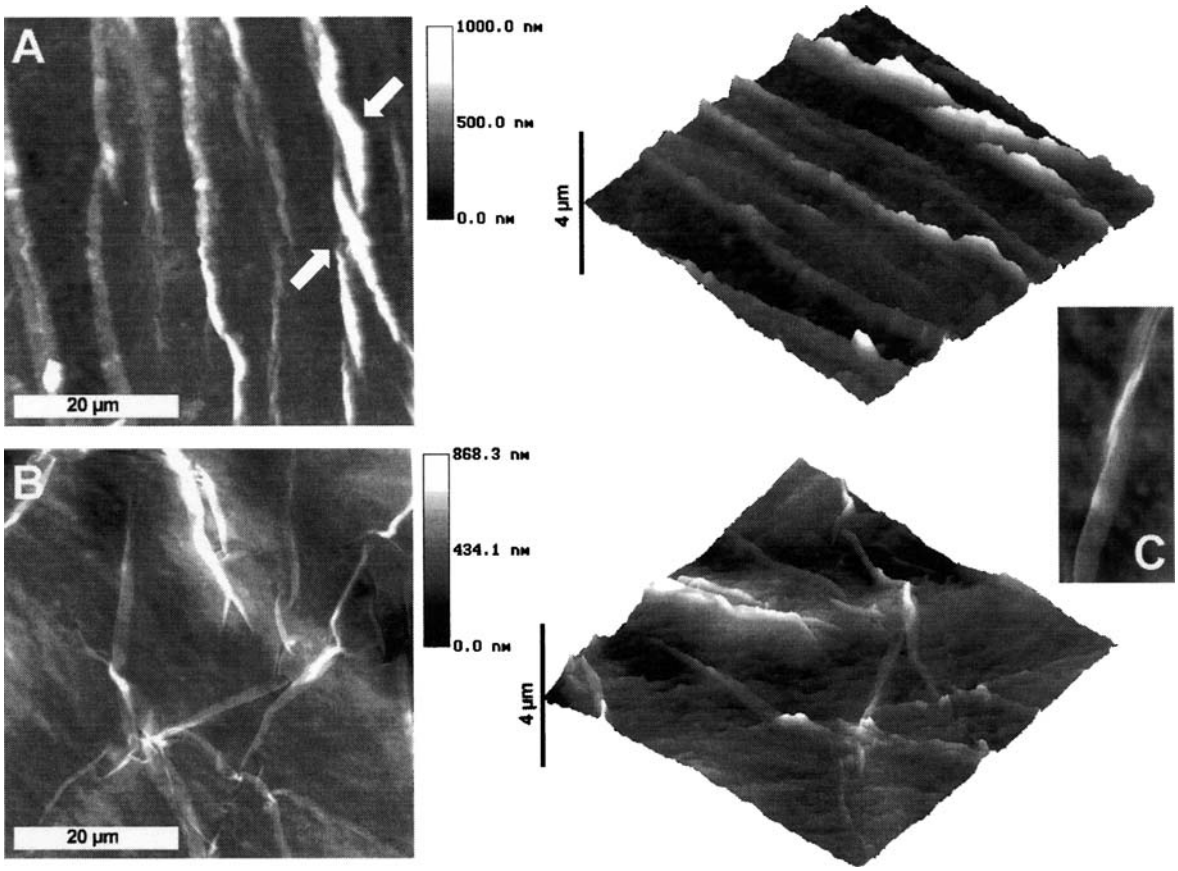

Fig. 2 Atomic force microscopy images of a κ-carrageenan/chitosan polyelectrolyte complex gel. The hydrogel samples were prepared under a spin rate (A), or under magnetic stirring (B). Detail of a κ-carrageenan/chitosan fibril (C). Bi-dimensional and three-dimensional views are shown. Note that the vertical scale of the 3D views is the same in both cases.

between the images of both types of samples clearly shows that the samples prepared by spin-coating, using spin rates higher than 100 rpm, display an ordered and oriented distribution of fibrils. In contrast, the magnetic stirred samples exhibit a random dispersion of fibrils. It should be noted that optical microscopy studies allowed us to get relevant morphological data on the effect of both sample preparation methods. In addition, the AFM technique, which a rather local character, was applied to characterize at higher resolution the fibril structures.

The previous characterization by optical microscopy was useful to select low roughness surface areas allowing their

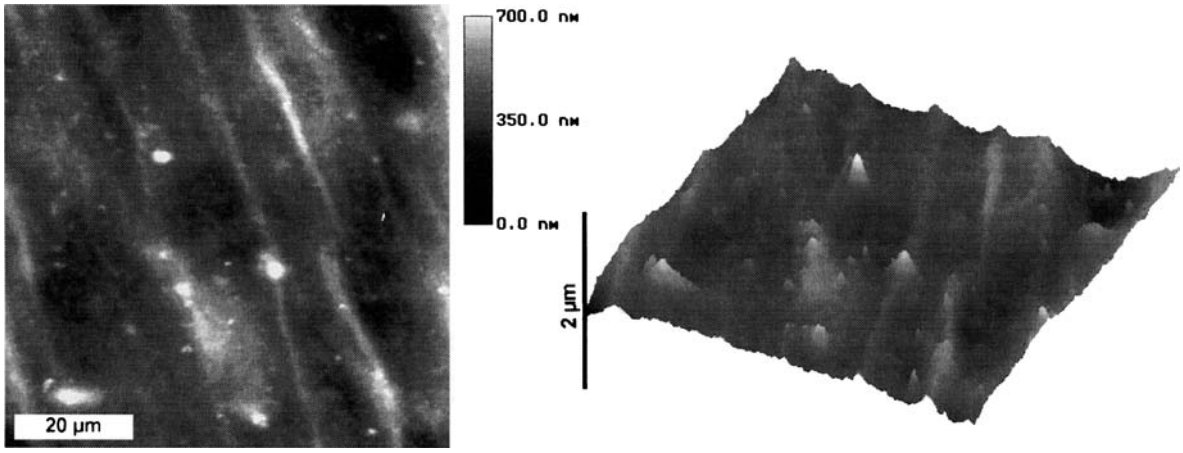

Fig. 3 Bidimensional and three-dimensional views of a fibrin gel prepared under spin coating conditions, analyzed by atomic force microscopy. Note that the vertical scale of the 3D view is half of that of the κ-carrageenan/chitosan gel.

further analysis by means of AFM. This last technique also showed the presence of domains where fibrils were arranged in parallel, perpendicularly to the applied centrifugal force (Fig. 2A), as well as the randomly arranged fibrils displayed in the gel samples prepared in the absence of centrifugal force (Fig. 2B). The AFM technique allowed both the measurement of the fibrils dimensions and the determination of their morphology. The fibrils formed under a centrifugal force (Fig. 2A) have a lateral size of 3–4 μm and a height in the 200-500 nm range. These fibrils seem to be bundled together (see arrows in Fig. 2A) and within the bundles the fibrils appear twisted. Both, twisting of individual fibrils and bundle morphology explain the wide range of the observed fibril dimensions. In addition, tip convolution effects may lead to overestimation of the fibril width. The average distance between neighboring fibrils, estimated from the peak in the power spectral density function of the image, was 5–7 μm.

In contrast, the fibrils observed in Figure 2B, showing the AFM image of the disordered gel formed under conventional magnetic stirring, are not aligned at all. They have a lateral dimension in the 1.5–3 micron range whereas the height is in the 150–300 nm range. Thus, they result to be smaller than those observed in Figure 2A. In this case, the fibrils are clearly twisted (Fig. 2C). Also, it is observed in Figure 2B that many of the fibrils are seen to emerge from the bulk of the sample suggesting a threedimensional network of fibrils not only at the surface but also beneath it. Finally, it is interesting to note that the fibrils of Figure 2B are flatter than those shown in Figure 2A since the root mean square roughness of the latter is twice that of the formers.

3.2. Fibrin gels oriented under dynamic conditions

The same procedure of gelation under dynamic conditions seems to be useful to induce order in a fibrin network, giving rise to transparent and stable gels with fibrils arranged in parallel, similarly to the κ-carrageenan/chitosan gel. In this case, polymerization was initiated by addition of thrombin to a fibrinogen solution in TBS containing $CaCl_2$. Thrombin catalyses the hydrolytic removal of fibrinopeptides A and B, converting fibrinogen into fibrin. Fibrin monomers are assembled by means of noncovalent interactions resulting in two-stranded protofibrils that aggregate laterally to form fibers. Usually these fibers branch into a three-dimensional network stabilized by covalent bonding in the presence of factor XIIIa [24], giving an opaque gel. However, when the polymerization process takes place under dynamic conditions, applying a spin rate of 450 rpm, atomic force microscopy confirms the presence of fibril domains arranged in parallel (Fig. 3).

The AFM image of fibrin gel shows the aggregation of fibrin fibrils in thicker strands arranged in parallel, 2.5 to 4 μm wide and 70–120 nm high. The average distance between fibrils is 10 to 15 microns, although it should be noted that they are not as periodically spaced as those observed in Fig. 2A.

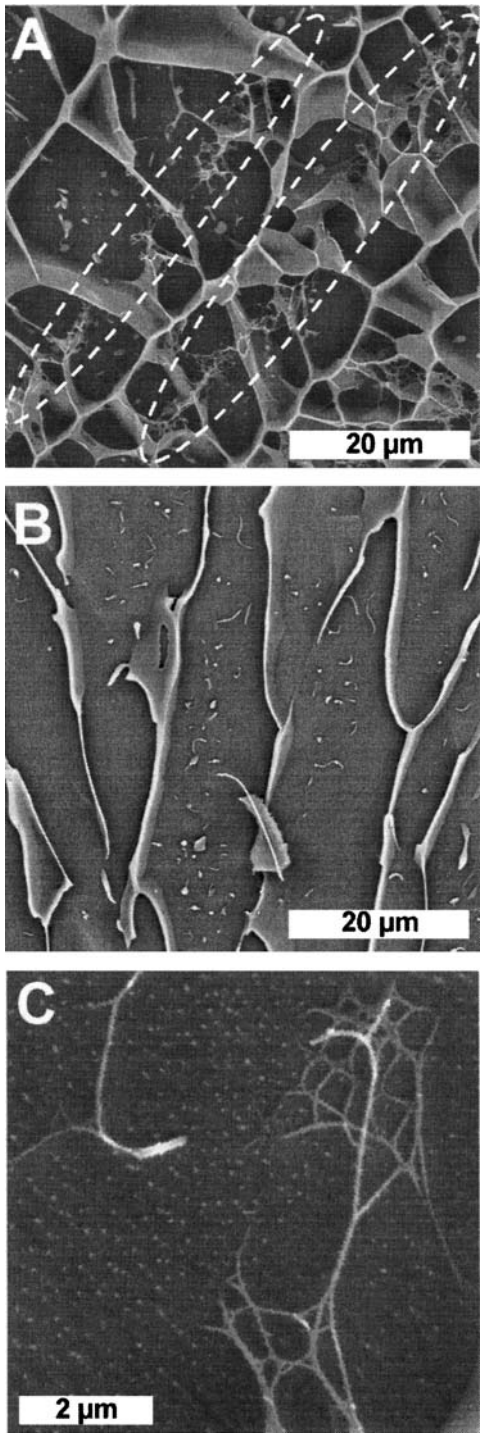

Fig. 4 Low temperature scanning electron microscopy images of a fibrin gel prepared from a mixture of fibrinogen, thrombin and $CaCl_2$ in TBS: (A), under centrifugal force; (B), the same reaction mixture without thrombin; (C) detail of a fibrin fibril.

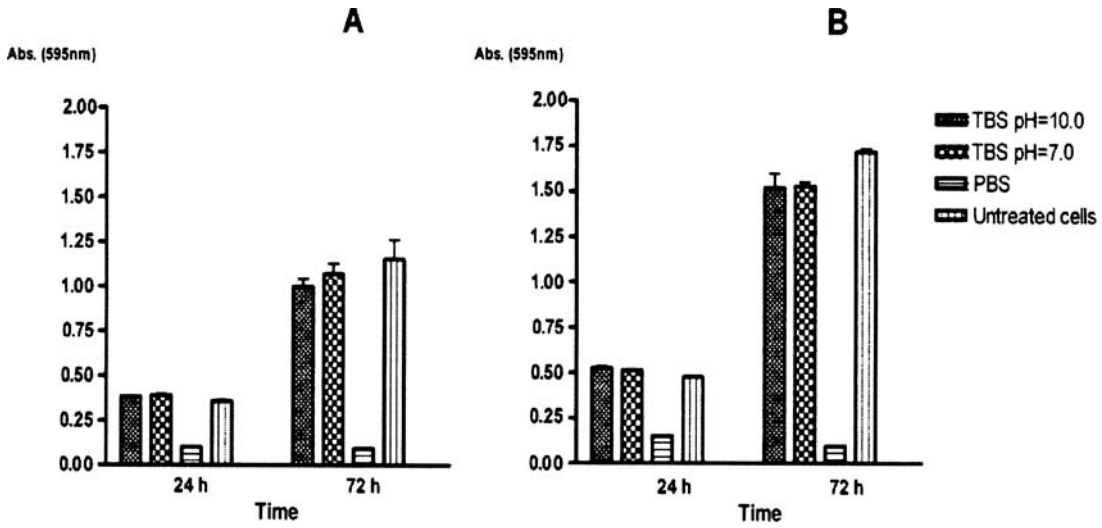

Fig. 5 The alkaline treatment does not affect the C6 cells viability. The C6 cells at 5×10^3 (A) or 10^4 cell per well (B) were treated by TBS at pH 10.0 or pH 7.0 and incubated for 24 and 72 h. A minimal reduction in cell viability in comparison to untreated cell was observed in both cases. Correlation between cell number seeded and the change in absorbance was maintained in the incubation periods assayed.

3.3. LTSEM imaging of oriented fibrin gel

The study of gel samples by AFM is quite difficult since gels must be dried. Even under such conditions the AFM measurements can be complicated due to the sample surface roughness induced by the drying process. For this reason, fibrin gel samples prepared under dynamic conditions have been also examined by means of LTSEM (Low Temperature Scanning Electron Microscopy). Using such technique, the samples can be imaged in a wet state, being the hydrogel structure preserved due to a freezing step by immersion in liquid N_2. Thus, the parallel display of the fibrin fibrils has been confirmed. In this way, the solid structure of water containing the electrolytes from the buffer solution can be also observed together with the fibrin fibrils. In Fig. 4 A, the fibrin fibrils, aggregated as linear and parallel fibers (encircled by white dashed lines), can be observed between the ice structures. In a blank sample, prepared in the same conditions but without addition of thrombin, the structures corresponding to the ice walls are also observed, the isolated proteins and dispersed salts being discerned between them (Fig. 4B). A detail of the fibrin fibrils is presented in Fig. 4C, and from this LTSEM image the diameter of the observed fibrils can be estimated in an average value of 75 nm, in good agreement with previous results reported by Ryan and coworkers [24]. Therefore, the parallel structures observed in Fig. 4A may result from the aggregation of fibrin fibrils in a preferred direction. The diameter of such aggregates, estimated from the LTSEM image, is 1.7–2.2 μm, and the distance between parallel fibers is approximately 15 μm, as previously observed in the AFM image. The fact that these oriented fibrils have been found on wet samples (i.e. not on dried samples) allows us to discard artifacts due to hydrogel drying as the origin of the fibril orientation.

3.4. C6 cells viability after alkaline treatment

The reaction to obtain large fibrin fibers implies the use of TBS at pH 10 [12], as detailed in the Materials and Methods section, and this incubation in alkaline environment could induce loss of cell viability or alterations in cell activity. To determine this effect, we studied C6 glioma cells at 2 different concentrations for 1 and 3 days after incubation in bidimensional cultures under alkaline conditions, obtaining a minimal reduction in the proliferation activity in treated cells in comparison to untreated control (Fig. 5). The presence of the hydrogel made difficult to study the cell proliferation activity inside fibrin gels of all cell population; however the maintenance of cell divisions in bidimensional cultures demonstrated an appropriated physiological activity of C6 cells after incubation under this alkaline conditions.

3.5. Cell ordering in an oriented fibrin gel

Several types of cells used for transplantation have the capacity to migrate and colonize the required anatomical site. However, as a therapy, transplantation may fail due to aggregation, inhibition by the environment, or attachment to an incorrect target. The inclusion of the cells into an oriented hydrogel could reduce these undesirable phenomena. A feature that is important to control is the cell distribution in the hydrogel. In order to study cell ordering inside a fibrin gel *in vitro*, we used a rat CNS glioma line. C6 glioma cells, labeled with a nuclear dye, were incorporated into

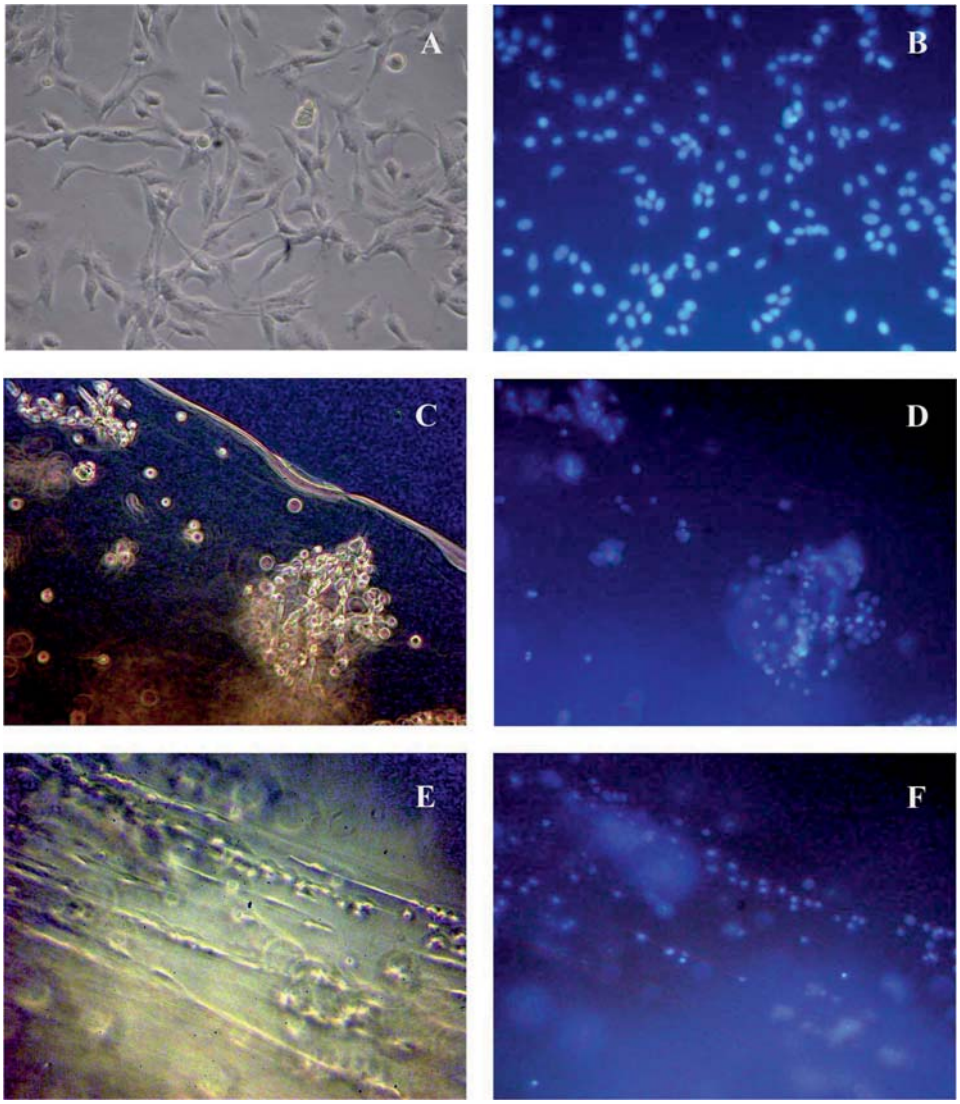

Fig. 6 Arranging cells by dynamic gelation. (A, B), C6 cells disposed themselves randomly on a bidimensional surface. (C, D), the cells assembled themselves in spherical globules inside a disordered fibrin gel. (E, F), However, when incorporated in fibrin gelating under centrifugal force, the cells differentiated processes and arranged themselves along the hydrogel fibrils. The nuclei (blue) show the position of the cells in the culture dish and in gels after culture for 12 h. Magnification, 200x.

fibrin fibrils gelated under centrifugal force. Their geometrical distribution was compared to C6 cells in bidimensional or tridimensional cultures (Fig. 6).

Glioma cells cultured over a bi-dimensional surface were distributed randomly (Fig 6A, B). When C6 cells were cultured inside a fibrin gel, they aggregated in spherical globules and individual cells did not differentiate any processes (Fig. 6 C, D). However cells incorporated during gelation under dynamic conditions become bipolar, aligning and elongating their processes in the direction of the fibrin gel (Fig. 6E, F). Gelation under these conditions strongly diminished cell aggregation, allowing a homogeneous distribution of differentiated cells inside the gel.

Biopolymers ordered as described above, with the inclusion of glial cells, may be useful as bridges for the reconnection of CNS neurons separated by injury; besides, ordered cellular bridges could create a well-distributed gradient of trophic factors, needed in damaged nerve tissue repair.

4. Conclusions

Experimental spinal cord lesions have been repaired by transplantation of glial cells [17, 20, 25, 26]. However, optimal tissue distribution, survival and function of transplanted cells, has not been assured. The work reported here opens the possibility of differentiating cells more uniformly inside a biocompatible gel. The inclusion of glial cells during ordered gelation yields a more controlled disposition and differentiation of the cells inside the gel, offering new possibilities of cellular manipulation *ex vivo* for transplantation in the CNS.

Acknowledgements This work was partially supported by the CICYT (Spain; Projects: MAT2003-06003-C02-01 and SAF-2002-04016-C02), the Comunidad Autónoma de Madrid (Spain; Project 07 N/0070/2002) and the CSIC (Spain, PIF Project 200460 F0320). E.D.-P. is supported by the Servicio de Salud de Castilla La Mancha Community (SESCAM). M. D. and E. M.-L. were supported by a postdoctoral I3 P contract (CSIC) and by a predoctoral fellowship from the

Comunidad Autónoma de Madrid, respectively. We thank F. Pinto for excellent technical assistance in LTSEM studies.

References

1. M. NIETO-SAMPEDRO, J. E. COLLAZOS-CASTRO, J. S. TAYLOR, G. GUDIÑO-CABRERA, E. VERDÚ-NAVARRO, J. I. PASCUAL-PIÉDROLA and R. INSAUSTI-SERRANO, Traumatic injuries to the central nervous system and their repair. *Rev Neurol* **35** (2002) 534–52.
2. Y. RAMÁN and S. CAJAL, Estudios sobre la degeneración y regeneración del sistema nervioso. Imprenta de Hijos de Nicolás Moya, Madrid, (1914).
3. P. M. RICHARDSON, U. M. McGUINNESS and A. J. AGUAYO, Axons from CNS neurons regenerate into PNS grafts. *Nature* **284** (1980) 264–65.
4. M. NIETO-SAMPEDRO, Neurite outgrowth inhibitors in gliotic tissue. *Advances Exper Med Biol* **468** (1999) 207–24.
5. J. L. GOLDBERG, M. P. KLASSEN, Y. HUA and B. A. BARRES, Amacrine-signaled loss of intrinsic axon growth ability by retinal ganglion cells. *Science* **296** (2002) 1860–4.
6. M. S. WIDMER and A. G. MIKOS, Fabrication of biodegradable polymer scaffolds for tissue engineering. Chapter II.5 in Frontiers in tissue engineering. JR C. W. PATRICK, A. G. MIKOS, L. V. MCINTIRE, Eds. Elsevier Science Ltd, UK, (1998) 106–20.
7. J. D. SIPE, C. A. KELLEY and L. A. McNICHOL, Eds. Reparative medicine: growing tissues and organs. Annals of the New York academy of sciences, New York, **961** (2002) 83–142.
8. H. M. GELLER and J. W. FAWCETT, Building a bridge: engineering spinal cord repair. *Exp Neurol* **174** (2002) 125–36.
9. G. W. PLANT, S. WOERLY and A. R. HARVEY, Hydrogels containing peptide or aminosugar sequences implanted into the rat brain: influence on cellular migration and axonal growth. *Exp Neurol* **143** (1997) 287–99.
10. S. WOERLY, E. PINET, L. de ROBERTIS, D. VAN DIEP and M. BOUSMINA, Spinal cord repair with PHPMA hydrogel containing RGD peptides (NeuroGel^{TM}). *Biomaterials* **22** (2001) 1095–111.
11. N. RANGAPPA, A. ROMERO, K. D. NELSON, R. C. EBERHART and G. M. SMITH, Laminin-coated poly(L-lactide) filaments induce robust neurite growth while providing directional orientation. *J Biomed Mater Res* **51** (2000) 625–34.
12. H. HALL, T. BAECHI and J. A. HUBBELL, Molecular properties of fibrin-based matrices for promotion of angiogenesis *in vitro*. *Microvasc Res.* **62** (2001) 315–26.
13. N. DUBEY, P. C. LETOURNEAU and R. T. TRANQUILLO, Neuronal contact guidance in magnetically aligned fibrin gels: effect of variation in gel mechano-structural properties. *Biomaterials* **22** (2001) 1065–75.
14. D. CEBALLOS, X. NAVARRO, N. DUBEY, G. WENDELSCHAFER-CRABB, W. R. KENNEDY and R. T. TRANQUILLO, Magnetically aligned collagen gel filling a collagen nerve guide improves peripheral nerve regeneration. *Exp Neurol* **158** (1999) 290–300.
15. N. DUBEY, P. C. LETOURNEAU and R. T. TRANQUILLO, Guided neurite elongation and Schwann cell invasion into magnetically aligned collagen in simulated peripheral nerve regeneration. *Exp Neurol* **158** (1999) 338–50.
16. L. BESSEAU, B. COULOMB, C. LEBRETON-DECOSTER and M. M. GIRAUD-GUILLE, Production of ordered collagen matrices for three-dimensional cell culture. *Biomaterials* **23** (2002) 27–36.
17. J. POLENTES, J. C. STAMEGNA, M. NIETO-SAMPEDRO and P. GAUTHIER, Phrenic rehabilitation and diaphragm recovery after cervical injury and transplantation of olfactory ensheathing cells. *Neurobiol Dis.* **16** (2004) 638–53.
18. Y. LI, T. CARLSTEDT, C. H. BERTHOLD and G. RAISMAN, Interaction of transplanted olfactory-ensheathing cells and host astrocytic processes provides a bridge for axons to regenerate across the dorsal root entry zone. *Exp Neurol* **188** (2004) 300–8.
19. J. S. RIDDELL, M. ENRIQUEZ-DENTON, A. TOFT, R. FAIRLESS and S. C. BARNETT, Olfactory ensheathing cell grafts have minimal influence on regeneration at the dorsal root entry zone following rhizotomy. *Glia* **47** (2004) 150–67.
20. M. NIETO-SAMPEDRO, Central nervous system lesions that can and those that cannot be repaired with the help of olfactory bulb ensheathing cell transplants. *Neurochem Res.* **28** (2003) 1659–76.
21. V. MUÑETÓN, S. AVERILL, V. KING, Q. YANG, E. DONCEL-PÉRÉZ, S. CABALLERO, R. WARD, M. NIETO-SAMPEDRO, J. PRIESTLEY and J. TAYLOR, Transplantation of olfactory ensheating cells fails to promote significant axonal regeneration from dorsal roots into the rat cervical cord. *J Neurocytol* **32** (2003) 53–70.
22. T. SAKIYAMA, C. H. CHU, T. FUJII and T. YANO, Preparation of a polyelectrolyte complex gel from chitosan and kappa-carrageenan and its ph-sensitive swelling. *J Appl Polym Sci.* **50** (1993) 2021–5.
23. T. SAKIYAMA, H. TAKATA, M. KIKUCHI and K. NAKANISHI, Polyelectrolyte complex gel with high pH-sensitivity prepared from dextran sulfate and chitosan. *J Appl Polym Sci.* **73** (1999) 2227–33.
24. E. A. RYAN, L. F. MOCKROS, J. W. WEISEL and L. LORAND, Structural origins of fibrin clot rheology. *Biophys J.* **77** (1999) 2813–26.
25. D. K. RESNICK, C. F. CECHVALA, Y. YAN, B. P. WITWER, D. SUN and S. ZHANG, Adult olfactory ensheathing cell transplantation for acute spinal cord injury. *J Neurotrauma* **20** (2003) 279–85.
26. E. VERDÚ, G. GARCIA-ALIAS, J. FORES, R. LOPEZ-VALES and X. NAVARRO, Olfactory ensheathing cells transplanted in lesioned spinal cord prevent loss of spinal cord parenchyma and promote functional recovery. *Glia* **42** (2003) 275–86.